

Eikonal Approximation in AdS/CFT : From Shock Waves to Four{Point Functions

Lorenzo Comalba^a, Miguel S. Costa^{b,c}, João Penedones^{b,c} and Ricardo Schiappa^d

^aDipartimento di Fisica & INFN, Università di Roma "Tor Vergata",
Via della Ricerca Scientifica 1, 00133, Roma, Italy

^bDepartamento de Física e Centro de Física do Porto,
Faculdade de Ciências da Universidade do Porto,
Rua do Campo Alegre, 687, 4169-007 Porto, Portugal

^cLaboratoire de Physique Théorique de l'École Normale Supérieure,
24 Rue Lhomond, 75231 Paris, France

^dTheory Division, Department of Physics, CERN,
CH-1211 Geneva 23, Switzerland

cornalba@roma2.infn.it, miguelc@fc.up.pt, jpenedones@fc.up.pt, ricardos@mail.cern.ch

Abstract: We initiate a program to generalize the standard eikonal approximation to compute amplitudes in Anti{de Sitter spacetimes. Inspired by the shock wave derivation of the eikonal amplitude in flat space, we study the two{point function $E(O_1 O_1)_{\text{shock}}$ in the presence of a shock wave in Anti{de Sitter, where O_1 is a scalar primary operator in the dual conformal field theory. At tree level in the gravitational coupling, we relate the shock two{point function E to the discontinuity across a kinematical branch cut of the conformal field theory four{point function $A(O_1 O_2 O_1 O_2)$, where O_2 creates the shock geometry in Anti{de Sitter. Finally, we extend the above results by computing E in the presence of shock waves along the horizon of Schwarzschild BTZ black holes. This work gives new tools for the study of Planckian physics in Anti{de Sitter spacetimes.

Keywords: AdS/CFT, Eikonal Approximation, 4{Point Functions, Shock Waves, BTZ Black Hole.

Contents

1. Introduction and Summary	2
2. Preliminaries and Notation	6
3. The Shock Wave Geometry	9
3.1 General Spin j Interaction	10
4. Two-Point Function in the Shock Wave Geometry	12
5. Creating the Shock Wave Geometry	14
6. Relation to the Dual CFT Four-Point Function	18
6.1 An Example in $d = 2$	22
7. Shock Wave in the BTZ Black Hole	23
8. Future Work	25
A. Propagators and Contact n -Point Functions	27
B. Explicit Computations in Poincare Coordinates	28

1. Introduction and Summary

The AdS_{d+1}/CFT_d correspondence relates, in general, a theory of strings on the negatively curved Anti-de Sitter (AdS) space with a conformal field theory (CFT) living on its boundary [1, 2, 3, 4]. When the radius ℓ of AdS_{d+1} is large compared with the string length ℓ_s , we can, in first approximation, analyze the dynamics of the low energy gravitational theory for the massless string modes. However, in most circumstances, we are forced to restrict our attention to tree level gravitational interactions, since the loop expansion in the gravitational coupling G is plagued with the usual ultraviolet (UV) problems present also in flat space, when we neglect the regulator length ℓ_s . In the prototypical example of the duality between type IIB strings on $AdS_5 \times S^5$ and $N = 4$ $U(N)$ supersymmetric Yang-Mills (SYM) theory in $d = 4$, the gravitational coupling in units of the AdS radius $G \ell^3$ is proportional to N^{-2} , and therefore we are in general forced to consider the planar limit of the SYM theory, even when the 't Hooft coupling $(\lambda \ell_s)^4$ is large. Moreover, even at tree level, Feynman graphs which are readily computed in flat space are extremely complex in AdS, limiting the practical use of the perturbative expansion [5, 6, 7].

In this paper we initiate a program to go beyond the tree level approximation and to explore the physics on AdS_{d+1} at finite $G \ell^{d-1}$. To do so, we recall that, in flat space M^{d+1} , the quantum effects of various types of interactions can be reliably resummed to all orders in the relevant coupling constant, in specific kinematical regimes [8, 9, 10, 11, 12, 13, 14]. In particular, the amplitude for the scattering of two particles can be approximately computed in the eikonal limit of small momentum transfer compared to the center-of-mass energy, or, equivalently, of small scattering angle. In this limit, even the gravitational interaction can be approximately evaluated to all orders in G , and the usual perturbative UV problems are rendered harmless by the resummation process. Moreover, at large energies, the gravitational interaction dominates all other interactions, quite independently of the underlying theory [9]. At high energies, scattering amplitudes in the eikonal limit exhibit a universal behavior which is indicative of the presence of gravity in the theory under consideration.

It is therefore tempting to speculate that, in certain favored kinematical regimes, quantum effects can be resummed also in AdS and that the gravitational interaction, if present, will dominate all other interactions and exhibit a universal behavior which will be a clear signal of the existence of a gravitational description in the dual CFT. This paper is a first step towards the consistent application of eikonal methods to the dynamics in AdS and to the physics of the dual CFT.

Let us start by recalling some basic facts about the eikonal formalism in flat space. Consider the scattering of two scalar particles in flat Minkowski space M^{d+1} . For the present purposes, we work at high energies and we neglect the masses of the scattering particles. The scattering amplitude A is a function of the Mandelstam invariants s and t and is computed in perturbation theory

$$A = A_0 + A_1 + \dots ;$$

where A_0 corresponds to graph (a) in figure 1 describing free propagation in spacetime. The tree level amplitude A_1 contains, in general, many different graphs. However, in the eikonal regime of small scattering angle $\theta \ll 1$, the t -channel exchange of massless particles dominates the full tree level amplitude. Therefore, the only relevant contribution to A_1 will come from graph (b) in figure 1, where j denotes the spin of the exchanged massless particle. More precisely, this contribution reads¹

$$A_1 \sim 4^{3-j} 2^{-j} i G \frac{s^j + c_1 s^{j-1} t + \dots + c_j t^j}{t} ;$$

¹The normalization $4^{3-j} 2^{-j} i G$ has been chosen for later convenience. When $j = 2$, the gravitational coupling constant G is the canonically normalized Newton constant.

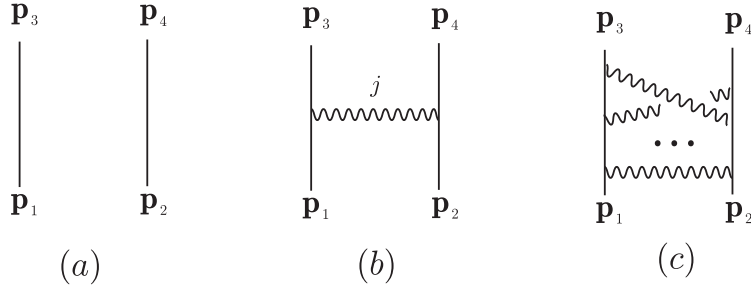


Figure 1: Interaction diagrams in both flat and AdS spaces. In the eikonal regime, free propagation (a) is modified primarily by interactions described by crossed-ladder graphs (c). In flat space and in this regime, the tree level amplitude is dominated by the t-channel graph (b) with maximal spin $j = 2$ of the exchanged massless particle. Moreover, the full eikonal amplitude can be computed from diagram (b).

In the eikonal limit, the full amplitude A is dominated by the ladder graphs (c) in figure 1 and can be reconstructed starting from A_1 . More precisely, we write A in the impact parameter representation

$$A(s; t) = \int_{E^{d-1}} d^2 q \int_{-\infty}^{\infty} ds e^{iq \cdot x} e^{2i(s;r)}; \quad (1.1)$$

where $r = \frac{p_\perp}{x^2}$ is the radial coordinate in transverse space E^{d-1} and q is the transverse momentum transfer. In general, the phase shift $\delta(s; r)$ receives contributions at all orders in perturbation theory. However, the leading behavior of $\delta(s; r)$ for large r is uniquely determined by the tree level interaction A_1 and is therefore obtained by a simple Fourier transform

$$A_1(s; t) = \int_{E^{d-1}} d^2 q \int_{-\infty}^{\infty} ds e^{iq \cdot x} \delta(s; r); \quad (1.2)$$

This yields

$$\delta(s; r) = 8G \frac{s^{j-1}}{4} \Delta(r);$$

where $\Delta(r)$ is the massless Euclidean propagator in transverse space E^{d-1} . The behavior of δ for large r is determined only by the residue of the $l=t$ pole in A_1 , and is insensitive to the other terms, proportional to c_i , which are regular for $t \neq 0$. Hence, the higher order graphs of figure 1 (c) are taken into account simply by exponentiating the phase δ in (1.1). In the limit of high energy s , the mediating massless particle with maximal spin j dominates the interaction. In theories of gravity, this particle is the graviton, with $j = 2$.

In the literature there are essentially two derivations of the eikonal amplitude (1.1). One derivation [8] considers the behavior of the Feynman diagrams in figure 1 (c) in the limit $t \ll s$, which, after a careful combinatorial analysis, re-sum to the result (1.1). The second derivation [9] is more geometrical and considers the motion of particle 1 in the classical field configuration created by particle 2. In the limit of large s , the particles move approximately at the speed of light, and particle 2 is viewed as a source, localized along its null worldline, for the exchanged massless spin j field. This classical source produces a shock wave configuration [15] in the exchanged field, and one may solve the wave equation for particle 1 in the presence of this classical background. When crossing the shock wave, the phase of the wave function for particle 1 is shifted by $2\delta(r; s)$ and the amplitude between the initial and final states of particle 1 is then given by the eikonal result (1.1).

In this work, we shall consider the CFT analogue of $2 \rightarrow 2$ scattering of scalar fields in flat space. More precisely, we will study the CFT correlator

$$\langle O_1(p_1) O_2(p_2) O_1(p_3) O_2(p_4) \rangle_{\text{CFT}_d} = \frac{1}{p_{13} p_{24}} A(z; z);$$

where the scalar primary operators O_1, O_2 have conformal dimensions Δ_1, Δ_2 , respectively. The p_i are now points on the boundary of AdS, and the amplitude A is a function of two cross-ratios z, \bar{z} (the precise definition of our notation can be found in section 2). Neglecting string effects, the function A can be computed in the dual AdS formulation as a field theoretic perturbation series [2, 3, 6, 7]

$$A = A_0 + A_1 + \dots;$$

where $A_0 = 1$ corresponds to free propagation described by the Witten diagram in figure 1(a). We expect that the eikonal kinematical regime in AdS is still defined by $p_1 \rightarrow p_3$, which corresponds to the limit of small cross-ratios z, \bar{z} . In analogy with flat space, we shall focus uniquely on the contribution to A_1 coming from the graph 1(b).

The direct generalization of the flat space eikonal resummation to AdS is not obvious, because AdS graphs are much harder to compute even at tree level [6, 7]. Fortunately, as described above, in flat space there is an alternative way to derive the eikonal result (1.1), which uses the shock wave geometry of the exchanged massless field. In this paper, we shall extend this analysis by considering the two-point function $E = \langle O_1 O_1 \rangle_{\text{shock}}$ on AdS_{d+1} in the presence of a shock wave of a spin j massless field. By analogy with flat space, we expect that the shock wave two-point function E contains contributions from all ladder graphs of figure 1. In particular, the first two terms in the coupling constant expansion

$$E = E_0 + E_1 + \dots;$$

should correspond, respectively, to free propagation and to tree level T -channel exchange of a spin j massless particle. Indeed, we shall determine a precise relation between E_1 and the tree level amplitude A_1 associated to graph 1(b). We will find that E_1 controls the small z, \bar{z} behavior of the discontinuity function (monodromy)

$$M_{-1}(z; \bar{z}) = \text{Disc}_z A_1(z; \bar{z}) - \frac{1}{2} \log \frac{A_1(z; \bar{z})}{A_1(\bar{z}; z)}; \quad (1.3)$$

where A_{-1} is the analytic continuation of A_1 obtained by keeping \bar{z} fixed and by transporting z clockwise around the point at infinity as in figure 2. More precisely, the small z, \bar{z} behavior of M_{-1} plays the role of the residue of the $1=t$ pole in A_1 in the flat space case and it is given by

$$M_{-1}(z; \bar{z}) \sim \left(\frac{z}{\bar{z}} \right)^j M \left(\frac{z}{\bar{z}} \right); \quad (1.4)$$

where the function $M(w)$ satisfies

$$M(w) = w^{1-j} M(1/w);$$

$$M(w)^2 = M(w^2);$$

Note that (1.4) is not directly related to the small z, \bar{z} behavior of A_1 , which is in turn controlled by the standard OPE in the dual CFT. As in flat space, the maximal spin j dominates in the eikonal regime of

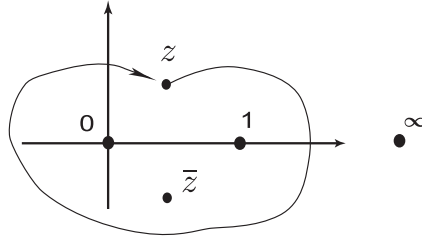


Figure 2: Analytic continuation of A_1 to obtain A_1 . The variable z is kept fixed and z is transported clockwise around the point at infinity, circling the points $0; 1; z$.

small $z; \bar{z}$. The leading behavior of M_1 is explicitly given as an integral representation over transverse space analogous to (1.2). As derived in section 6, we shall find that

$$M_1' = 8GN_1N_2 \int_{H_{d-1}} \frac{d^2x d^2y}{Z} \frac{(x;y)}{(2q^2 - \vec{x}^2)^{1+1+j} (2p^2 - \vec{y}^2)^{2-1+j}}; \quad (1.5)$$

where the relevant notation is given in detail in section 2. In a companion paper [16] we will explore the CFT consequences of the above result.

One crucial step is missing to complete the eikonal program. In flat space, one can approximately reconstruct the full amplitude from the tree level phase shift using (1.1). This last step cannot be immediately done in AdS_{d+1} , since the tree level eikonal two-point function E_1 is not related to A_1 but rather to the discontinuity M_1 of A_1 across a kinematical branch cut. Therefore, in order to reconstruct A_1 and the full amplitude A from the shock wave two-point function, extra information is needed. In [16] we shall conjecture a possible resolution of this problem, even though more work is needed to put these results on firm grounds.

Let us further comment on the above result, and on its relation to the more familiar flat space case. In the CFT literature, one usually considers the amplitude $A_1(z; \bar{z})$ evaluated on the principal Euclidean sheet, where $z = z^2$ (again see section 2 for a precise definition of the notation). It is quite clear, on the other hand, that eikonal results, both in flat and in AdS space, probe amplitudes deep in the Lorentzian regime. In fact, scattered particles are almost lightlike separated in position space, due to the high relative energies. Therefore, in the context of the AdS/CFT duality, we must also consider the boundary CFT correlator $A_1(z; \bar{z})$ in its Lorentzian regime. This is obtained by analytically continuing $A_1(z; \bar{z})$, with $z; \bar{z}$ now viewed as independent variables. The channel $z; \bar{z} \neq 0$ corresponds to lightlike separation of the relevant scattering particles but, as explained in detail in section 5, this limit must be accompanied by the relevant analytic continuation in (1.3). Note that, implicitly, this continuation is also performed in the flat space eikonal computation, but it is immaterial in this case since, in momentum space, tree level amplitudes are rational functions of the kinematical invariants. Finally, let us note that, without analytic continuation, the limit of A_1 for $z; \bar{z} \neq 0$ goes like z^j ^{Energy} and is therefore governed by the usual OPE. In this case, the relevant contribution comes from only a finite number of states of lowest energy propagating in this channel. This corresponds to the state O_j dual to the spin j particle being exchanged, and the eikonal result would amount to a computation of the three-point coupling $\langle h_{10} h_{10} h_{j0} \rangle$. The eikonal result, on the other hand, contains much more information. The limit $z; \bar{z} \neq 0$ of M_1 goes in

fact like $|j\rangle^{\text{spin}}$ and we obtain information about the full tower of spin j intermediate states, which is encoded in the generating function $M(w)$.

Finally, in section 7, we extend the computation of the two-point function $E_{hO_1O_1}^{\text{shock}}$ to the case of a shock wave propagating along the horizon of a Schwarzschild BTZ black hole [17, 18]. This computation extends the results of [19, 20, 21, 22, 23], where CFT correlators are used to extract information on the physics behind the horizon of the black hole, with particular emphasis on the singularity. In particular, in future work we plan to relate E to the four-point function in the BTZ geometry at all orders in G , thus probing the physics of the singularity in a truly quantum gravity regime.

In two appendices, we further include a full discussion on the AdS and Hyperbolic space propagators required in the main text; and an explicit calculation of the shock two-point function, in the case of $d = 3$, using Poincare coordinates. This will provide the reader who is familiar with the correlation function calculations of [3, 24] a simpler access to the calculations we perform in the bulk of the paper.

2. Preliminaries and Notation

Recall that AdS_{d+1} space, of dimension $d+1$, can be defined as a pseudo-sphere in the embedding space $M^2 \times M^d$. We denote with $x = (x^+, x^-, x)$ a point in $M^2 \times M^d$, where x^\pm are light cone coordinates on M^2 and x denotes a point in M^d . Then, AdS space of radius ℓ is described by ²

$$x^2 = -x^+x^- + x^2 = -\ell^2 \quad (2.1)$$

Similarly, a point on the holographic boundary of AdS_{d+1} can be described by a ray on the light cone in $M^2 \times M^d$, that is by a point p with

$$p^2 = -p^+p^- + p^2 = 0;$$

defined up to rescaling

$$p \rightarrow \lambda p \quad (\lambda > 0):$$

In figure 3 the embedding of the AdS geometry is represented for the AdS_2 case. From now on we choose units such that $\ell = 1$.

The AdS/CFT correspondence predicts the existence of a dual CFT_d living on the boundary of AdS_{d+1} . In particular, a CFT correlator of scalar primary operators located at points $p_1; \dots; p_n$, can be conveniently described by an amplitude

$$A(p_1; \dots; p_n)$$

invariant under $SO(2; d)$ and therefore only a function of the invariants

$$p_{ij} = 2p_i \cdot p_j$$

Since the boundary points p_i are defined only up to rescaling, the amplitude A will be homogeneous in each entry

$$A(\dots; p_i; \dots) = \lambda_i^{-\Delta_i} A(\dots; p_i; \dots);$$

where Δ_i is the conformal dimension of the i th scalar primary operator.

²We denote with $x \cdot y$ and $x \cdot y$ the scalar products in $M^2 \times M^d$ and M^d , respectively. Moreover, we abbreviate $x^2 = x \cdot x$ and $x^2 = x \cdot x$ when clear from context. In M^d we shall use coordinates x with $x^0; \dots; x^{d-1}$ and with x^0 the timelike coordinate. Finally, in M^2 we shall write $x = x^{d+1} \cdot x^d$ for the light cone coordinates, with x^{d+1} the time direction and x^d the spatial one.

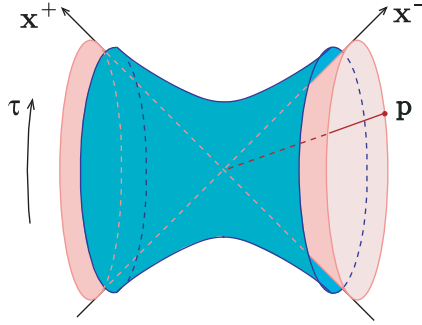


Figure 3: Embedding of AdS_2 in $M^2 \times M^1$. A point p in the boundary of AdS_2 is a null ray in $M^2 \times M^1$.

Throughout this paper we will focus our attention on four-point amplitudes of scalar primary operators. More precisely, we shall consider correlators of the form

$$A(p_1; p_2; p_3; p_4) = \langle O_1(p_1) O_2(p_2) O_1(p_3) O_2(p_4) \rangle_{CFT_d}$$

where the scalar operators $O_1; O_2$ have dimensions

$$\Delta_1 = \Delta + \ell; \quad \Delta_2 = \Delta - \ell;$$

respectively. The four-point amplitude A is just a function of two cross-ratios $z; \bar{z}$ which we define, following [25, 26], in terms of the kinematical invariants p_{ij} as³

$$z \bar{z} = \frac{p_{13} p_{24}}{p_{12} p_{34}}; \\ (1-z)(1-\bar{z}) = \frac{p_{14} p_{23}}{p_{12} p_{34}};$$

Then, the four-point amplitude can be written as

$$A(p_i) = \frac{1}{p_{13}^{\Delta_1} p_{24}^{\Delta_2}} A(z; \bar{z});$$

where A is a generic function of $z; \bar{z}$. By conformal invariance, we can fix the position of up to three of the external points p_i . In what follows, we shall often choose the external kinematics by placing the four points p_i at

$$\begin{aligned} p_1 &= (0; 1; 0); & p_2 &= (1; p^2; p); \\ p_3 &= (q^2; 1; q); & p_4 &= (1; 0; 0); \end{aligned} \quad (2.2)$$

and we shall view the amplitude as a function of $p; q \in M^d$. The cross-ratios $z; \bar{z}$ are in particular determined by

$$z \bar{z} = q^2 p^2; \quad z + \bar{z} = 2p \cdot q;$$

³Throughout the paper, we shall consider barred and unbarred variables as independent, with complex conjugation denoted by $\bar{}$. In general $z = \bar{z}^2$ when considering the analytic continuation of the CFT_d to Euclidean signature. For Lorentzian signature, either $z = \bar{z}^2$ or both z and \bar{z} are real. These facts follow simply from solving the quadratic equations for z and \bar{z} .

When $d = 2$ it is convenient to parameterize M^d by light cone coordinates $x = x^0 + x^1$ and $x = x^0 - x^1$, with metric $dx dx$. Then, if we choose $p = p = 1$ we have $q = z, q = z$.

In the sequel, we will denote with $H_{d-1} \subset M^d$ the transverse hyperbolic space, given by the upper mass shell

$$x^2 = 1 \quad x^0 > 0 ;$$

where $x \in M^d$. We will also denote with $M^+ \subset M^d$ the future Milne wedge given by $x^2 \geq 0, x^0 \geq 0$. Similarly, we denote with M^- the past Milne wedge and with H_{d-1} the associated transverse hyperbolic space. Finally we denote with

$$\tilde{dx} = 2dx \sqrt{x^2 + 1} ;$$

$$\tilde{dx} = 2dx \sqrt{x^2 + 1} ;$$

the volume elements on AdS_{d+1} and H_{d-1} , respectively. For example

$$\int_M dx = \int_0^Z t^{d-1} dt \int_{H_{d-1}} \tilde{dy} ;$$

where $x = ty$ and $y \in H_{d-1}$.

Throughout the paper, we will often need the massless Minkowskian scalar propagator $\Delta(x; y)$ on AdS_{d+1} and the massive Euclidean scalar propagator $\Delta(x; y)$ on H_{d-1} of mass squared m^2 . They are canonically normalized by

$$\int_{AdS_{d+1}} \Delta(x; y) = i \int_{H_{d-1}} \Delta(x; y) = (d-1) \int_{H_{d-1}} \Delta(x; y) ;$$

and are explicitly given in appendix A. We also introduce, for future use, the constant N given by the integral

$$N^{-1} = \int_M \frac{dy}{\sqrt{y}^{d-2}} e^{2k \cdot y} = (2) \int_{H_{d-1}} \frac{\tilde{dy}}{(2k \cdot y)^2} = \frac{d-1}{2} \int_{H_{d-1}} \frac{\tilde{dy}}{(2k \cdot y)^2} ;$$

To conclude this section, let us remind the reader that we have been careless about the global structure of AdS_{d+1} . As it is well known, the locus (2.1) has a non-contractible timelike circle, and we shall denote with \tilde{AdS}_{d+1} the covering space of (2.1), where global time, given by

$$x^{d+1} + ix^0 = \frac{1}{2} (x^+ + x^-) + ix^0 = \cosh(\tau) e^i ; \tag{2.3}$$

is decomposed. Therefore, one must be cautious when working in the embedding coordinates since two general bulk points x and x^0 , or two boundary points p and p^0 , related by a global time translation of integer multiples of 2π have the same embedding in $M^2 \subset M^d$. Given a boundary point p , we may divide the AdS space in an infinite sequence of Poincare patches separated by the null surfaces $x - p = 0$ and labeled by integers n increasing as we move forward in global time. The $n = 0$ patch is the one which is spacelike related to the boundary point, as shown in figure 4. These global issues will be relevant in sections 4 and 5.

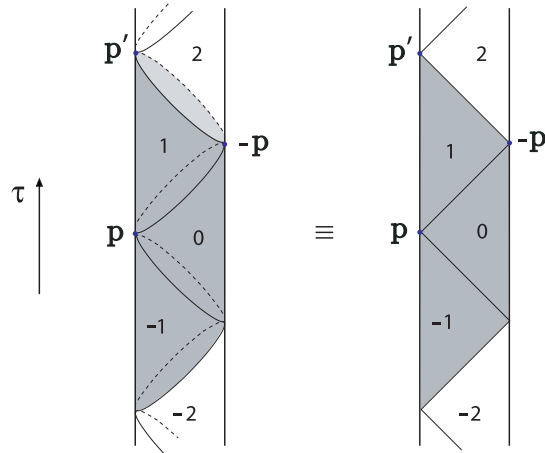


Figure 4: Poincare patches of an arbitrary boundary point p , separated by the null surfaces $2x - p = 0$. Here AdS is represented as a cylinder with boundary $R = S_{d-1}$. Throughout this paper we shall mostly use a two-dimensional simplification of this picture, as shown in the figure. The point p and an image point p^0 of p are also shown.

3. The Shock Wave Geometry

In this section we review the shock wave geometry in AdS_{d+1} , which is a direct analog of the Aichelburg-Sexl geometry in flat space and which has been described in [27, 28, 29, 30, 31, 32].

In order to easily describe the geometry, it is convenient to focus first on two consecutive Poincare patches in AdS_{d+1} with $x > 0$ and $x < 0$, respectively. As shown in figure 5, these two regions are separated by the surface in AdS_{d+1} defined by $x = 0$ and are parameterized by the light cone coordinate x^+ and by a point x in the transverse hyperbolic space H_{d-1} . Since the two Poincare patches are invariant under translations generated by $x^- \partial_- + 2x^+ \partial_+$, we may parameterize the $x < 0$ patch with new coordinates

$$\begin{aligned} x^+ &= 2x^+ + x^2 x^-; \\ x^- &= x^-; \\ x &= x; \end{aligned}$$

where $2x^+ M^d$ is arbitrary. We may then think of the two patches as being described by different coordinate systems glued along the surface $x = 0$ with the following gluing conditions

$$\begin{aligned} x^+ &\rightarrow x^+ + h(x); \\ x^- &\rightarrow x^-; \end{aligned} \tag{3.1}$$

where

$$h(x) = 2x^+ x^-.$$

As we move from one patch to the next, the light cone coordinate x^+ is shifted by an amount $h(x)$ which depends only on the transverse coordinates $x \in H_{d-1}$. Moreover, note that the function $h(x)$ satisfies

$$\int_{H_{d-1}} (d-1) h = 0; \tag{3.2}$$

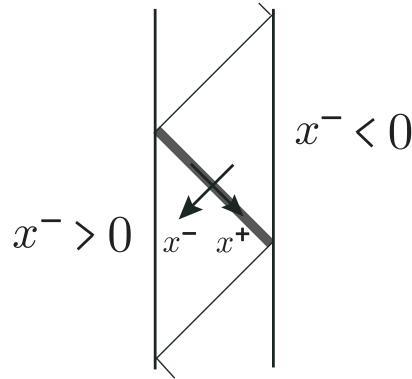


Figure 5: Two consecutive Poincaré patches with $x^- > 0$ and $x^- < 0$. The shock geometry can be described by specifying gluing conditions on the separating surface $x = 0$, which is parameterized by x^+ and x^- , with $x^2 \in H_{d-1}$.

To show this fact, recall that any function $h(x)$ defined on a (pseudo) Euclidean space E^{D+2} which is harmonic and homogeneous, i.e., $\nabla_{E^{D+2}}^2 h = 0$ and $h(\lambda x) = \lambda^m h(x)$, satisfies, when restricted to the (pseudo) sphere S_{D+1} given by $x^2 = 1$, the equation $\nabla_{S_{D+1}}^2 h = 0$, where $m^2 = (D-1)$.

Up to now we have only described the original AdS_{d+1} space using different coordinate systems in different parts of the space. The geometry describing a shock wave propagating along the surface $x = 0$ is obtained by adding, to the vacuum Einstein equations, a source term localized at $x = 0$ and independent of the null coordinate x^+ . The shock geometry can then be easily described by gluing two AdS_{d+1} patches as in (3.1). As explained below, the gluing function now satisfies (3.2) with a source term on the right-hand side of the equation given by

$$16 G T(x);$$

where $x^2 \in H_{d-1}$ and G is the Newton constant measured in units of the AdS radius. We denote as usual with $\Delta(x; y)$ the Euclidean scalar propagator of mass $d-1$ in the transverse space H_{d-1} , canonically normalized so that

$$\nabla_{H_{d-1}}^2 \Delta(x; y) = -\Delta(x; y);$$

and given explicitly in appendix A. In the presence of a source term $T(x)$ the gluing function $h(x)$ is then given by

$$h(x) = 16 G \int_{H_{d-1}} \Delta(x; x^0) T(x^0); \quad (3.3)$$

The usual AdS AdS geometry can then be recovered by choosing a source due to a particle of energy E localized in transverse space at $y \in H_{d-1}$

$$T(x) = E \Delta(x; y);$$

$$h(x) = 16 G E \Delta(x; y);$$

3.1 General Spin j Interaction

An equivalent way to present the shock wave geometry is to note that, as in flat space, the linear response of the metric to a stress-energy tensor localized along a null surface actually solves the full non-linear gravity equations. In this case, the full metric reads

$$ds^2(AdS_{d+1}) + dx^2 h(x);$$

where h is localized on the shock front at $x = 0$ and depends only on the transverse directions x^2, \dots, x^d .

$$h(x) = \delta(x) h(x) :$$

The metric deformation h is generated by a stress-energy tensor

$$T(x) = \delta(x) T(x) ; \tag{3.4}$$

located along the shock front. Einstein's equations

$$\Delta_{\text{ds}_{d+1}} h = 16 G T$$

again translate, in transverse space, to

$$\Delta_{\text{H}_{d-1}} (d-1) h = 16 G T ;$$

which is solved by (3.3).

We now wish to consider the propagation of a complex scalar field ϕ of mass m in the presence of the shock. The metric deformation h changes the free Lagrangian

$$Z = \int d^d x \frac{1}{2} \partial_\mu \phi^\dagger \partial^\mu \phi - m^2 \phi^\dagger \phi$$

by adding them in in gravitational coupling $\frac{R}{4} \int d^d x \frac{1}{2} \partial_\mu \phi^\dagger \partial^\mu \phi$, where we used that the only non-vanishing component of the metric fluctuations is $h_{\mu\nu} = h \delta_{\mu\nu}$. For the purposes of this paper, we will need to consider a more general interaction mediated by a spin j particle. We may still consider a classical probe for h localized on the null surface $x = 0$ as described above, but now associated to a shock wave of the spin j massless field. The interaction with the scalar field will then be of the more general form

$$Z = \int d^d x \frac{1}{4} \partial_\mu \phi^\dagger \partial^\mu \phi + \int d^d x \frac{1}{2} \partial_\mu \phi^\dagger \partial^\mu \phi h ; \tag{3.5}$$

where now h is the component $h_{\mu\nu}$ of the spin j field. The equations of motion for ϕ then read

$$m^2 \phi = 4 h \partial_\mu \phi^\dagger \partial^\mu \phi = 4 \partial_\mu \phi^\dagger \partial^\mu \phi h ; \tag{3.6}$$

which translate in a boundary condition for ϕ at the location of the shock. Around $x = 0$ the differential equation (3.6) simplifies to

$$\partial_+ \partial_- \phi = \partial_\mu \phi^\dagger \partial^\mu \phi h ;$$

Taking the Fourier transform $\int dx^+ e^{ix^+ s}$ with respect to x^+ , we obtain

$$\partial_- \ln \phi(s; x^-) = \partial_\mu \phi^\dagger \partial^\mu \phi (is)^{j-1} h(x) ;$$

Therefore, the value of the field ϕ changes across the shock according to

$$\phi(x^+, x^-) = e^{h(x) (is)^{j-1}} \phi(x^+, x^-) ; \tag{3.7}$$

In particular, for $j = 2$ we recover the previous result $\phi(x^+, x^-) = e^{h(x)} \phi(x^+, x^-)$ in (3.1).

4. Two-Point Function in the Shock Wave Geometry

We are now in the position to compute the two-point function of the scalar field ϕ in the presence of the shock. From now on we shall view the field ϕ as dual to the operator O_ϕ of conformal dimension Δ_ϕ , with $\Delta_\phi(\phi) = m_\phi^2$, and we shall be interested in its boundary to boundary correlator.

Recall first the standard bulk to boundary propagator $K_{p_1}(x)$ of ϕ , from a boundary point p_1 to a bulk point x in the absence of the shock (3.1). It is given by $C_\phi (2x - p_1)^{-\Delta_\phi}$, where⁴

$$C_\phi = \frac{1}{2^{\frac{d}{2}}} \frac{\Gamma(\frac{d}{2})}{\Gamma(\frac{d}{2} + 1)}$$

and where we must pay particular attention to the exact phase factor. More precisely, as described at the end of section 2, given the boundary point p_1 , the AdS space may be divided in an infinite sequence of Poincaré patches separated by the surfaces $2x - p_1 = 0$ and labeled by integers n increasing as we move forward in global time. The $n = 0$ patch is the one which is spacelike related to the boundary point, as shown in figure 4. Then, the correct definition of the bulk to boundary propagator is

$$K_{p_1}(x) = C_\phi \frac{i^{2-j} \Gamma(j)}{\Gamma(x - p_1)^j} : \quad (4.1)$$

We shall mostly concentrate on the three patches labeled by $n = 0$; -1 and shown in grey in figure 4, where we can also write

$$K_{p_1}(x) = \frac{C_\phi}{(\Gamma(x - p_1 + i))^j} : \quad (4.2)$$

Let us stress that (4.2) is not valid in general. In fact, had we extended (4.2) throughout the whole AdS space, we would have the propagator from a collection of boundary points related to p_1 and $-p_1$ by 2 translations in global time.

Now we compute the two-point function between boundary points p_1 and p_3 in the presence of a shock wave, where p_1 is on the boundary of the patch preceding the shock, as shown in figure 6. Using translations $x \rightarrow x + 2x_{\text{shock}}$ in this patch, we are free to place the point p_1 at

$$p_1 = (0; 1; 0) ;$$

so that the relevant bulk to boundary function is given, before the shock, by

$$\frac{C_\phi}{(\Gamma(x^+ + i))^j} = \frac{i^{2-j} C_\phi}{(\Gamma(x^+))^j} \int_0^1 ds s^{-j} e^{isx^+} :$$

Just after the shock, using the gluing relation (3.7), the scalar profile becomes

$$\frac{i^{2-j} C_\phi}{(\Gamma(x^+))^j} \int_0^1 ds s^{-j} e^{isx^+ + (is)^j h(x)} : \quad (4.3)$$

⁴The normalization C_ϕ is not the standard one used in the literature [5, 3]. In this paper, the bulk to boundary propagator $K_{p_1}(x)$ is taken to be the limit of the bulk to bulk propagator $G(x; y)$ as the bulk point y approaches the boundary point p_1 . As shown in [33, 24] and briefly in appendix B, naive Feynman graphs in AdS computed with this prescription give correctly normalized CFT correlators, including the subtle two-point function.

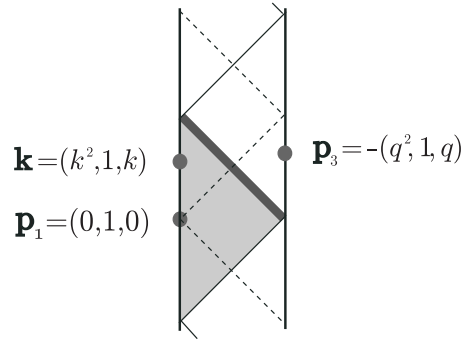


Figure 6: Computation of the two-point function between the boundary points p_1 and p_3 in the presence of a shock along the thick diagonal line. This is equivalent to a linear superposition of propagators from k to p_3 in the absence of the shock, where the boundary point k runs over the grey patch $x^- > 0$. We have divided the AdS space in patches along the $x^- = 0$ surface (continuous lines, including the shock surface) and along the $x^+ = 0$ surface (dashed lines).

We want to write the above function, defined on the shock surface $x^- = 0$, as a coherent sum

$$C_{13} = \int \frac{dk}{(2\pi)^d} \frac{F(k)}{(x^+ - 2k - x^- + i\epsilon)^d} \quad (4.4)$$

of bulk to boundary propagators $K_k(x)$ where, as shown in figure 6, the point $k = (k^2; 1; k)$ runs over the boundary of the patch preceding the shock. To determine $F(k)$ we equate the Fourier transforms with respect to x^+ of (4.3) and (4.4) and obtain, for $s > 0$,

$$e^{(is)^{d-1}h(x)} = \int \frac{dk}{(2\pi)^d} F(k) e^{2ik \cdot (sx)}.$$

This equation may now be inverted by considering sx as a point in the future Minkowski wedge M^+ , decomposed in its radial and angular parts. We then obtain

$$F(k) = 2^d \int_0^\infty s^{d-1} ds \int_{H_{d-1}} dx e^{2ik \cdot (sx) + (is)^{d-1}h(x)}. \quad (4.5)$$

Having obtained the scalar profile (4.4) just after the shock, we may now evolve it forward after the surface $x^- = 0$ and compute the boundary to boundary correlator E , by considering the limit of the profile

$$\int \frac{dk}{(2\pi)^d} F(k) K_k(x) \quad (4.6)$$

as the point x moves towards the boundary point

$$p_3 = (q^2; 1; q)$$

in the patch after the shock. We need to be careful with phases using the general form of the propagator (4.1) since p_3 can be outside the $n = 0; -1$ Poincare patches of k , as shown in figure 7. More precisely, one arrives at the following integral

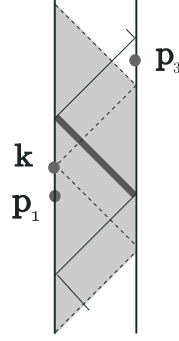


Figure 7: In expression (4.6), we are not allowed to use (4.2) for the bulk to boundary propagator. In fact, the point p_3 , limiting boundary point of x , is not always inside the $n = 0; -1$ patches of point k , which are shown in grey. In general, p_3 is within the $n = 0; 1; 2$ patches of k .

$$E = C_{-1} \int \frac{dk}{(2)^d} \frac{F(k)}{[(k^2 - q^2) + i \text{sign}(k^0 - q^0)]^{-1}} :$$

Using (4.5) and changing variables to $k^0 = s(k^2 - q^2)$ we obtain

$$E = i^{2-j} C_{-1} \int_0^1 s^{2-j-1} ds \int_{H_{d-1}} \int_{H_{d-1}} \frac{dx}{dx} e^{2iq \cdot (sx) + (is)^j h(x)} \int \frac{dk^0}{d} \frac{e^{2ik^0 \cdot x}}{[k^2 - i \text{sign}(k^0)]^{-1}} :$$

The last integral in the above expression is a constant since $x \in H_{d-1}$. This constant can be evaluated, for example, by considering the limit $h = 0$ with $q^2 = M^2$ in the past Minkowski wedge. In this case E is given by the free propagator $C_{-1} q^2^{-1}$, thus showing that the constant is given by N_{-1} . We have then arrived at the final result

$$E = i^{2-j} C_{-1} N_{-1} \int_0^1 s^{2-j-1} ds \int_{H_{d-1}} \int_{H_{d-1}} dx e^{2iq \cdot (sx) + (is)^j h(x)} :$$

When $j = 2$ the s integral can be easily performed to obtain

$$E = C_{-1} N_{-1} (2)^{-1} \int_{H_{d-1}} \frac{dx}{(2q \cdot x + h(x) + i^2)^1} ; \quad (j = 2) : \quad (4.7)$$

5. Creating the Shock Wave Geometry

In flat space the computation analogous to the previous section yields a non-perturbative approximation to the four-point amplitude in the eikonal kinematic regime. To understand the relation between the AdS result of the previous section and the dual CFT four-point function, we consider the tree level term in the expansion of the two-point function E in powers of h

$$\begin{aligned} E_1 &= (i)^{j-1} C_{-1} N_{-1} (2)^{-1+j-1} \int_{H_{d-1}} \int_{H_{d-1}} \frac{dx}{dx} \frac{h(x)}{(2q \cdot x + i^2)^{1+j-1}} \\ &= 16 G (i)^{j-1} C_{-1} N_{-1} (2)^{-1+j-1} \int_{H_{d-1}} \int_{H_{d-1}} \frac{dx}{dx} \frac{dy}{dy} \frac{(x; y) T(y)}{(2q \cdot x + i^2)^{1+j-1}} : \end{aligned} \quad (5.1)$$

In this section, we shall show that the function E_1 can also be computed from the Feynman graph in figure 1 (b), which corresponds to a tree level exchange of a massless spin j particle between two scalar particles ϕ_1 and ϕ_2 , with appropriate external wave functions. The fields ϕ_i have masses m_i and are dual to boundary operators O_i of conformal dimension Δ_i . Moreover, the relevant coupling for the field ϕ_2 , parallel to (3.5), is given by ⁵

$$Z = \int d^d x \phi_2^j h^0; \quad (5.2)$$

where h^0 is the h_+ component of the interaction spin j field, which has a two-point function

$$h(x)h^0(x^0) = 8G_N x; x^0;$$

The massless scalar propagator in AdS_{d+1} is canonically normalized by $\langle \phi(x; x^0) \phi(x'; x'^0) \rangle = i \delta(x; x^0)$ and it is explicitly given in appendix A. We will denote with $\phi_1; \phi_3$ and $\phi_2; \phi_4$ the external wave functions of the AdS graph corresponding, respectively, to the two fields ϕ_1 and ϕ_2 interacting through the massless exchange. In general the external states $\phi_1; \phi_3$ and $\phi_2; \phi_4$ will be linear combinations of the bulk to boundary propagators

$$K_p(x) = C_1 (2x - p)^1;$$

$$\tilde{K}_p(x) = C_2 (2x - p)^2;$$

respectively. Throughout this section, we will fix the external states $\phi_1; \phi_3$ to be

$$\phi_1 = K_{p_1}; \quad \phi_3 = K_{p_3};$$

according to the previous section⁶. If we also choose

$$\phi_2 = \tilde{K}_{p_2}; \quad \phi_4 = \tilde{K}_{p_4};$$

the graph 1 (b) computes the amplitude $C_1 C_2 A_1(p_i) = C_1 C_2 p_{13}^{-1} p_{24}^{-2} A_1(p_i)$. However, we shall choose the wave functions $\phi_2; \phi_4$ so that the corresponding vertex (5.2), schematically given by $\phi_2^j \phi_4$, is localized along the shock surface $x = 0$ and only along the x^0 direction. In other words, the wave functions ϕ_2 and ϕ_4 will be chosen such that the vertex (5.2) is the source for the shock wave. This will be achieved by choosing ϕ_2 and ϕ_4 to be a particular linear combinations of the basic external wave functions \tilde{K}_p . More precisely, the fields ϕ_2 and ϕ_4 will respectively vanish after and before the shock, so that their overlap $\phi_2^j \phi_4$ is supported only at $x = 0$. Moreover, near $x^0 = 0$, the functions ϕ_2 and ϕ_4 will be respectively chosen to behave in the light cone directions x^0 as $(x^0)^{2+j-1}$ and $(x^0)^{-2}$, so that their overlap $\phi_2^j \phi_4$ goes as $1 = x^0(x^0)$. With this specific choice of external states $\phi_2; \phi_4$, graph 1 (b) is explicitly given by

$$Z = \int_{AdS_{d+1}} d^d x \phi_3^j \phi_4 h(x);$$

⁵The sign $(-)^j$ indicates that, for odd j , the fields ϕ_1 and ϕ_2 are oppositely charged with respect to the spin j interaction field. With this convention, graph 1 (b) corresponds to an attractive interaction, independently of j .

⁶In this section, all external states ϕ_i are built starting from the canonical bulk to boundary propagator (4.1). This includes the states ϕ_2, ϕ_4 used to explicitly construct the shock wave. The phase conventions in (4.1) show that the bulk to boundary propagator $K_p(x)$ corresponds to a non-normalizable wave with a δ function source at the boundary point p . Computation of Feynman integrals with those external states corresponds then, in the dual CFT, to a computation of the boundary correlator in the relevant Lorentzian regime. Note, finally, that the phases in (4.1) are obtained by a canonical Wick rotation in global time, starting from Euclidean AdS in global coordinates.

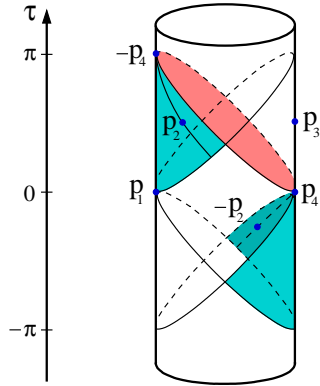


Figure 8: Construction of the external wave functions ψ_2 and ψ_4 starting from the bulk to boundary propagators K_{p_2} and K_{p_4} . The points p_4 are fixed, whereas the points p_2 are free to move in the past null wedges (shaded regions of the boundary). In particular, in (5.8), the points p_2 lie along a ray from the origin, as shown. The source points p_1, p_3 are as in figure 6. We also show global AdS time.

where

$$h(x) = 16 G \int_{\text{AdS}_{d+1}} dx^0 \quad x; x^0 T \quad x^0 ; \quad (5.3)$$

$$T = \int_4 \partial^j \psi_2 :$$

As discussed above, the functions $\psi_2; \psi_4$ are chosen so that the source function T is supported on the light cone $T(x) = \delta(x) T(x)$, and the graph 1(b) computes E_1 for the specific choice of transverse source $T(x)$.

Following figure 8, we start by choosing as external state ψ_4 the linear combination

$$\psi_4 = i^2 \int K_{p_4} - K_{p_4} = C \int_2 (x - i)^2 - (x + i)^2 ; \quad (5.4)$$

where we chose $p_4 = (1; 0; 0)$. The wave function ψ_4 clearly vanishes before the shock for $x > 0$. Similarly, the function ψ_2 will be given by the general linear combination

$$\psi_2 = \int \frac{dp}{(2\pi)^d} G(p) K_{p_2} - \int i^2 K_{p_2} ; \quad (5.5)$$

where we write $p_2 = (1; p^2; p)$. The integrand in (5.5) vanishes for $x - p < 0$, so that, for $G(p)$ supported in the past null wedge M , the wave function ψ_2 vanishes after the shock for $x < 0$. Recall that we are interested in the overlap $\int_4 \partial^j \psi_2$, so that we need only the behavior of ψ_2 for $x > 0$. This in turn is controlled only by $G(p)$ for $p > 0$. To show this, we shall for a moment assume that $G(p)$ in (5.5) is homogeneous in p as $G(p) = \int G(p)$. Then ψ_2 is an eigenfunction of $x^+ \partial_+$ as follows

$$\int_2 (x^+; x; x) = \int c^{-2+d} \int_2 (x^+; x; x) ;$$

and behaves, close to $x = 0$, as

$$\int_2 (x^+; x; x) \sim (x)^c \int c^{-2+d} \int_2 (0; 1; x) ;$$

where $x \in H_{d-1}$. In general, we shall take, for reasons which shall become clear shortly,

$$G(p) = G_0(p) + \dots ;$$

$$G_0(p) = 2^{-(2+j-d-1)} G_0(p) ;$$

where the dots denote sub-leading terms for $p \rightarrow 0$. The above discussion then immediately implies that the behavior of ϕ_2 just before the shock is given by

$$\phi_2(x^+) = i^j \phi_2(x^-) + 2^{-(2+j-1)} g(x) + \dots ;$$

where x is a position in transverse space H_{d-1} and where $g(x)$ is determined uniquely by $G_0(p)$.

We are now in a position to explicitly compute the source term T in (5.3). We first recall the following representation of the delta function

$$\delta(x) = \int_{-\infty}^{\infty} \frac{d\lambda}{2\pi} e^{i\lambda x} = \int_0^{\infty} \frac{d\lambda}{2\pi} [e^{i\lambda x} + e^{-i\lambda x}] ;$$

$$= \int_0^{\infty} \frac{d\lambda}{2\pi} e^{-\lambda|x|} ; \quad \begin{matrix} (\lambda > 0) \\ (\lambda < 0) \end{matrix} ;$$

Writing the leading behavior of ϕ_2 as

$$\phi_2(x) = \frac{(2+j-1)!}{2^j} \int_0^{\infty} dt t^{j-1} e^{-t|x|} g(x) ;$$

and using the above representation of $\delta(x)$ we conclude that the source function T in (5.3) is given by

$$T(x) = \int_{-\infty}^{\infty} dx' T(x') ;$$

$$T(x) = (i^j)^{-1} 2^{-j} \int_0^{\infty} dt t^{j-1} g(x) ;$$

To explicitly compute the function $g(x)$ in terms of the weight function $G_0(p)$, we must simply evaluate (5.5) at $(0; 1; x)$, with G replaced by G_0 . The first term in (5.5) gives

$$C_2 \int_{-\infty}^{\infty} \frac{dp}{(2\pi)^d} \frac{G_0(p)}{(1+2p-x+i\epsilon)}$$

$$= \frac{C_2 i^{j-1}}{(2\pi)^d} \int_0^{\infty} dt t^{j-1} \int_{-\infty}^{\infty} \frac{dp}{(2\pi)^d} G_0(p) e^{i\epsilon(1+2p-x)}$$

$$= \frac{C_2 i^{j-1}}{2^{2+j-1}} \frac{(1-2-j)}{(2\pi)^d} G_0(x) ;$$

where we abuse notation and denote with $G_0(x) = (2\pi)^{-d} \int dp e^{ip \cdot x} G_0(p)$ the Fourier transform of $G_0(p)$. The second term in (5.5) is similarly given by

$$i^{2-j} C_2 \int_{-\infty}^{\infty} \frac{dp}{(2\pi)^d} \frac{G_0(p)}{(1-2p-x+i\epsilon)} = \frac{C_2 i^{1-j}}{2^{2+j-1}} \frac{(1-2-j)}{(2\pi)^d} G_0(x) ;$$

Note that, in this case, the i^+ prescription is correct since $G_0(p)$ is supported only in the past M line wedge M^- . We finally conclude that the T (channel exchange Witten diagram 1(b) with external wave functions ϕ_4 and ϕ_2 , respectively as in (5.4) and (5.5), is given by (5.1) with

$$T(x) = \frac{2 C_2^2}{2^{2+2+j-1}} \frac{(1-2)^h}{(2)} i^j G_0(x) + i^j G_0(x) ; \quad (5.6)$$

where recall that we are interested in $x \in H_{d-1}$. Denoting with A_1 the tree level correlator associated to graph 1(b) when the external points are at p_1, p_3 and p_2, p_4 , the same Witten diagram can be written as

$$E_1 = C_1 C_2 \int \frac{dp}{(2)^d} G(p) i^{2-2} A_1^+ + i^{2-2} A_1^+ A_1^{++} i^{4-2} A_1 : \quad (5.7)$$

It is particularly convenient to choose a weight function $G(p)$ supported along a straight line as shown in figure 8

$$G(p) = \int_0^a dt t^{2+2+j-2} (2)^{d-d} (p-\hat{p}t) ; \quad (5.8)$$

with $\hat{p} \in H_{d-1}$ a unit vector. Note that the behavior of $G(p)$ for $p \rightarrow 0$ is independent of a , and the leading behavior $G_0(p)$ is obtained by setting $a = 1$ in (5.8). We then have

$$G_0(x) = i^{2+2+j-1} \frac{(2-2+j-1)}{(\hat{p} \cdot x + i^2)^{2+j-1}} ;$$

and finally, for $x \in H_{d-1}$,

$$T(x) = (i)^{j-1} C_2 N_2 (2-2+j-1) \frac{1}{(2\hat{p} \cdot x)^{2+j-1}} ;$$

For this particular source the two-point function (5.1) becomes

$$E_1 = 16^{-2} G C_1 C_2 N_1 N_2 (2-1+j-1) (2-2+j-1) \int_{H_{d-1}} \frac{dx dy}{(2q \cdot x)^{1+j-1} (2\hat{p} \cdot y)^{2+j-1}} (x;y) ; \quad (5.9)$$

where we recall that both $q \cdot x$ and $\hat{p} \cdot y$ are positive if q is in the past M line wedge M^- .

6. Relation to the Dual CFT Four-Point Function

In this section we shall express the Lorentzian four-point correlators in (5.7) in terms of the Euclidean four-point function by means of analytic continuation. We will denote with $A_1(z; z)$ the Lorentzian amplitudes corresponding to the tree level correlators A_1 . More precisely, we have

$$A_1 = \frac{i^{2-1} \dot{p}_{13} \dot{p}_1^{2-2} \dot{p}_{24}^j}{\dot{p}_{13}^{j-1} \dot{p}_{24}^{j-2}} A_1 :$$

We have been careful with the exact phases and introduced, as in the discussion of the bulk to boundary propagator in section (4), the integer numbers n_{ij} which label the Poincare patch, relative to point p_i , containing the point p_j . Note that the cross-ratios z, \bar{z} are invariant under re-scalings $p_i \rightarrow \lambda_i p_i$ with

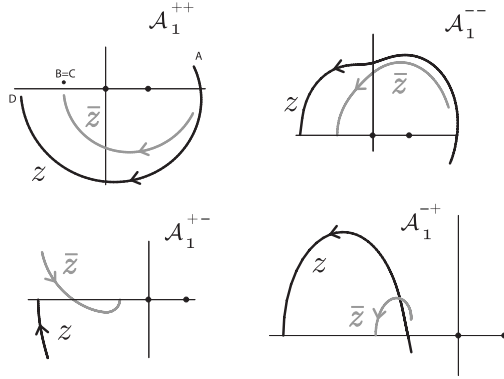


Figure 9: Wick rotation of z, \bar{z} when the external points are at p_1, p_3, p_2, p_4 . On the Euclidean principal sheet of the amplitude we have $z = z^2$ (initial points of the curves), while after Wick rotating to the Lorentzian domain $z; \bar{z}$ are real and negative (final points). Points A, B, C and D refer to the detailed analysis of A_1^{++} in figure 10.

α_i arbitrary, and in particular they are independent of the choice of signs in p_2, p_4 . This means that the functions $A_1(z; \bar{z})$ are given by specific analytic continuations of the basic Euclidean four-point amplitude $A_1(z; z)$.

Without loss of generality we may fix from now on $q^2 = M^2$. Recalling that $G(p)$ is non-vanishing only for $p^2 = M^2$, we have that $n_{13} = 0, n_{24}^{++} = 0, n_{24} = 2, n_{24}^+ = n_{24}^- = 1$. Therefore we can write (5.7) as

$$E_1 = C_1 C_2 \int_{\mathcal{Z}} \frac{dp}{(2\pi)^d} \frac{G(p)}{(\hat{q}^2 - p^2)^2} A_1^+ + A_1^- + A_1^{++} + A_1^{--};$$

where we recall that $z; \bar{z}$ are implicitly defined by

$$z \bar{z} = \hat{q}^2 p^2; \quad z + \bar{z} = 2\hat{q} \cdot p;$$

In particular, choosing $\hat{q} = \hat{q}^2 = H_{d-1}$ of unit norm and $G(p)$ as in (5.8), we obtain the expression

$$E_1 = C_1 C_2 \int_0^{\mathcal{Z}_a} dt t^{j-2} A_1^+ + A_1^- + A_1^{++} + A_1^{--}; \quad (6.1)$$

where now

$$\begin{aligned} z &= tw^{1=2}; & \bar{z} &= tw^{1=2}; \\ w^{1=2} + w^{-1=2} &= 2\hat{q} \cdot \hat{p}; \end{aligned} \quad (6.2)$$

Notice that for $\hat{q}; \hat{p} \in H_{d-1}$ we have that $\hat{q} \cdot \hat{p} = 1$ and therefore both z and \bar{z} are real and negative. We now must consider more carefully the issue of the analytic continuation. Consider a generic boundary point p , and let σ be the decomposed global time. We have that

$$\begin{aligned} p^{d+1} &= \cos(\sigma); \\ p^0 &= \sin(\sigma); \end{aligned}$$

In particular, denoting with $\theta_1, \theta_3, \theta_2, \theta_4$ the global times of the four boundary points p_1, p_3, p_2, p_4 , we clearly have that (see figure 8)

$$\begin{aligned} \theta_1 &= \theta_4 = 0; \\ \theta_3 &= \theta_2 + \pi; \\ \theta_1 &= \theta_3 + \pi; \\ \theta_2 &= \theta_4 + \pi. \end{aligned}$$

We can then consider, for each of the boundary points under consideration, the standard Wick rotation $t \rightarrow i\tau$ parameterized by $\alpha \in [0, 1]$

$$\begin{aligned} p^{d+1} &= \cos \alpha \, i \, \vec{e}^i; \\ p^0 &= \sin \alpha \, i \, \vec{e}^i; \end{aligned}$$

where $\alpha = 0$ corresponds to the Euclidean regime and $\alpha = 1$ to the Minkowski setting. In particular, given the four points p_1, p_3, p_2, p_4 , we may follow the cross(ratios $z(\alpha), \bar{z}(\alpha)$) as a function of α . The plots of $z(\alpha), \bar{z}(\alpha)$ in the four cases A_{\pm}^{\pm} are shown in figure 9. Note that, in the Euclidean limit, we have that

$$z(0) = (\bar{z}(0))^2;$$

as expected. On the other hand, when $\alpha = 1$, the cross(ratios $z(1), \bar{z}(1)$) are explicitly given by (6.2). We remark that, although figure 9 has been derived with a specific choice of $p = t\hat{p}$ and $q = \hat{q}$, the qualitative features of the curves are independent of the chosen p, q . Moreover, from figure 9, we deduce that

$$\begin{aligned} A_1^{++}(z; \bar{z}) &= A_1(z - i; \bar{z} - i); \\ A_1^+(z; \bar{z}) &= A_1(z - i; \bar{z} + i); \\ A_1^{-}(z; \bar{z}) &= A_1(z + i; \bar{z} + i); \\ A_1^-(z; \bar{z}) &= A_1(z + i; \bar{z} - i); \end{aligned}$$

where $A_{\pm}^{\pm}(z; \bar{z})$ is the analytic continuation of the Euclidean amplitude A_1 obtained by keeping z fixed and by transporting \bar{z} clockwise (counterclockwise) around the point at infinity. We explain the above result by concentrating on the first case of A_1^{++} . Consider the black curve $z(\alpha)$ in figure 9 for A_1^{++} . It can be deformed without crossing any singularity to the black curve in figure 10, which is composed of three parts AB, BC and CD. The first part AB is just the complex conjugate of the curve $z(\alpha)$. Therefore, at point B, we are clearly on the principal sheet A_1 . The curve BC, on the other hand, rotates clockwise around the point at 1 , moving therefore to the sheet A_1 . Finally the last segment CD is immaterial, since the function A_1 is only singular at $z = 0; 1; \bar{z}$.

In general we have that the Euclidean amplitude is real, in the sense that

$$A_1(z; \bar{z}) = A_1(\bar{z}; z); \quad A_1^2(z; \bar{z}) = A_1(z^2; \bar{z}^2);$$

Therefore

$$A_1^2(z; \bar{z}) = A_1(z^2; \bar{z}^2);$$

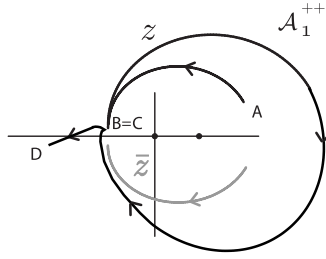


Figure 10: The black curve going through points A, B, C, D is obtained from a continuous deformation of the curve $z(\cdot)$ in figure 9 for A_1^{++} . It shows the relation of A_1^{++} with the Euclidean amplitude A_1 .

We then conclude that

$$A_1^+ + A_1^+ = A_1^{++} - A_1 = 4 \operatorname{Im} M_1(z - i; z - i);$$

where M_1 is the discontinuity function of A_1 defined in the introduction. Thus, the right hand side of (6.1) is explicitly given by

$$4 C_1 C_2 \int_0^a dt t^{j-2} \operatorname{Im} M_1(tw^{1=2}; tw^{-1=2}); \quad (6.3)$$

Recall from the discussion in the previous section that the above integral is independent of a . Therefore, the integrand is supported at $t = 0$, and the leading behavior of M_1 is given by

$$M_1(z; z) \sim (z^{-1})^j M \frac{z}{z}; \quad (6.4)$$

with $M^2(w) = M(w^2)$. Note, in particular, that the residue function $M(w)$ must be real in order for the integrand in (6.3) to be localized at $t = 0$, which follows from the independence of the integral on the upper limit of integration a . Then (6.3) becomes

$$4 C_1 C_2 w^{\frac{j-1}{2}} M(w) \int_0^a dt \operatorname{Im} \frac{1}{t+i} = 2^2 C_1 C_2 w^{\frac{j-1}{2}} M(w);$$

The two-point function E_1 is, on the other hand, given by (5.9) with $q = \frac{1}{2} H_{d-1}$. This gives then an integral representation for $M(w)$

$$w^{\frac{j-1}{2}} M(w) = \int_{H_{d-1}} \frac{dx dy}{(2q - x^2)^{1+j} (2p - y^2)^{2-1+j}} \frac{(x; y)}{Z}; \quad (6.5)$$

where we recall that $w^{1=2} + w^{-1=2} = 2q - p$. Clearly we have that

$$M(w) = w^{1-j} M \frac{1}{w};$$

Finally, using (6.4) and (6.5), we obtain the equivalent result (1.5) for the leading behavior of M_1 given in the introduction.

6.1 An Example in $d = 2$

Let us conclude this section with a simple example where we can check our result. We shall consider the case $j = 0$ corresponding to massless scalar exchange in AdS. The basic amplitude A_1 is given by

$$\frac{C_1 C_2}{P_{13} P_{24}} A_1 = 4i \int_{\text{AdS}_{d+1}} \frac{C_1^2}{(2x_1 \phi^1 (2x_3 \phi^1)} h(x);$$

where

$$h(x) = 32i \int_{\text{AdS}_{d+1}} \frac{C_2^2}{(2y_2 \phi^2 (2y_4 \phi^2)} (x; y)$$

and where $(x; y)$ is the massless propagator in AdS_{d+1} . We shall concentrate, in particular, on the simple case $d = 2$, so that the scalar field dual to the operator O_2 is massless in AdS_3 . In this case we can use the general technique in [34] and easily compute

$$h(x) = \frac{1}{(2)^2} \frac{8G}{P_{24} (2x_2 \phi (2x_4 \phi)};$$

where we have used $C = 1 = (2)$ for $d = 2$. In terms of the standard functions

$$D_i^d(p_i) = \int_{H_{d+1}} \frac{dx}{(2x_i \phi^i)};$$

reviewed in appendix A, we conclude, after Wick rotation

$$\int_{\text{AdS}_{d+1}} dx \int_{H_{d+1}} dx;$$

that

$$A_1 = \frac{8G}{P_{13} P_{24}} D_{1;1;1;1}^2(p_1; p_3; p_2; p_4); \tag{6.6}$$

We may also explicitly compute the integral (1.5), which controls the leading behavior as $z; z \rightarrow 0$ of $M_1 = D_{1;1;1;1}^2 A_1$. For $d = 2, j = 0$ we can use again the methods of [34] to explicitly perform the y -integral in (1.5). We then arrive at the result

$$M_1' = 8G \frac{(2-1-1)}{(1)^2} q^2 p^2 D_{2-1;1;1}^0(q; p);$$

Using the explicit form of $D_{2-1;1;1}^0$ given in appendix A, we conclude that $M_1' = zM(z=z)$, where the function $M(w)$ is explicitly given by

$$M(w) = \frac{4G}{2-1-1} w F_{1;1;2-1-1}(w); \tag{6.7}$$

where F is the standard hypergeometric function.

Furthermore, we shall restrict our attention to the special case $d = 2$, where the amplitude (6.6) can be explicitly computed [35]

$$A_1(z; z) = 8G \frac{z^2 z^2}{(z-z)} \frac{1}{1-z} \frac{1}{z} \frac{1}{1-z} a(z; z);$$

with

$$a(z; z) = \frac{(1-z)(1-z)}{(z-z)} \text{Li}_2(z) - \text{Li}_2(z) + \frac{1}{2} \ln(z-z) \ln \frac{1-z}{1-z}$$

and where $\text{Li}_2(z)$ is the dilogarithm. It is easy to check that $a(z; z) = a(z^{-1}; z^{-1})$, so that we quickly deduce that

$$\text{Disc}_z a(z; z) = \frac{1}{2} \frac{(1-z)(1-z)}{(z-z)} \ln \frac{1-z}{1-z} :$$

Applying to $\text{Disc}_z a$ the differential operator relating a with A_1 , we obtain an exact expression for the discontinuity of A_1

$$M_1 = 4G \frac{z-z}{(z-z)^3} z^2 \left(\frac{1}{2} + \ln \frac{1-z}{1-z} \right) - 2z-z - z^2-z - z^2-z :$$

For small $z; z$ the above expression simplifies to $M_1' = zM(z=z)$, with

$$M(w) = 4G \frac{w}{(1-w)^3} \left(\frac{1}{2} + 2w \ln(w) \right) - w^2 :$$

This is exactly (6.7) for $\nu_1 = 2$.

7. Shock Wave in the BTZ Black Hole

In this final section, we will extend the previous analysis of the two-point function in the presence of a shock to the case of the Schwarzschild BTZ black hole. Therefore, throughout this section, we shall work in $d = 2$. The main interest of this calculation is to understand, within the BTZ black hole example, how spacelike singularities and horizons can be described in terms of CFT amplitudes. This problem was first addressed in [36], where the BTZ geometry is conjectured to be dual to an entangled state between two copies of the CFT located at the two disconnected BTZ boundaries, and later further explored in [19, 20, 21, 22, 23]. In particular, the main goal of [19] is to extract, from CFT correlators, information on the physics behind the horizon, with particular emphasis on the singularity. One can probe physics behind the horizon by studying the two-point function $\langle O_1(p_1)O_1(p_3) \rangle$ of a boundary operator, where the boundary points are located on the two distinct BTZ asymptotic boundaries. In the case where this operator creates a bulk scalar particle with a large mass m_1 (and therefore large conformal dimension) one may evaluate the two-point function in the semiclassical geodesic approximation as [19]

$$\langle O_1(p_1)O_1(p_3) \rangle \sim \exp(-m_1 L) ;$$

where L is the (regularized) proper length of the spacelike geodesic which connects the two boundary points. Such a correlator gives access to the full spacetime, including the region behind the horizon. Extensions of these ideas in $d = 5$ were carried out in [20, 21]. On a different line [37], these two-point functions may also be used in the computation of greybody factors for BTZ black holes.

In what follows, we shall extend the results of [19] and compute the two-point function in the presence of a shock wave along the black hole horizon. As for the pure AdS case, this should be related to a specific kinematical regime, dominated by gravitational exchange, of the full four-point function in the entangled thermal state of the CFT. Therefore, this computation contains non-perturbative information about the dual CFT, which is probed, beyond the semiclassical gravitational regime, at finite G . These results could then allow us to study, following reasonings along the lines of [19, 20, 21], the physics of the singularity in

a full quantum gravity regime. We shall leave a full investigation of these issues to future work, limiting ourselves to the computation of the shock two-point function.

As described in section 2, Anti-de Sitter space AdS_3 is given by the $M^2 \times M^2$ embedding

$$x^2 = x^+ x^- + x x = 1;$$

where we use light cone coordinates $x; x$ on the second M^2 . As is well known [17, 18], the Schwarzschild BTZ black hole is described by the identifications

$$x \sim e x; \quad x \sim e x; \tag{7.1}$$

where e is related to the black hole mass M by $e = 2 \sqrt{\frac{p}{M}}$. The region outside the horizon, with $x > 0$ and $x^+ < 0$, can be parameterized with coordinates $r; t$ as

$$\begin{aligned} x &= e^t \sqrt{r^2 - 1}; \\ x &= r e; \\ x &= r e; \end{aligned} \tag{7.2}$$

with metric

$$ds^2 = -r^2 dt^2 + \frac{dr^2}{r^2 - 1} + r^2 d\phi^2;$$

The BTZ identification (7.1) simply amounts to the periodicity $\phi \sim \phi + 2\pi$.

The identifications (7.1) clearly leave the surface $x = 0$ invariant, and therefore we may still construct a shock geometry along the horizon by considering the gluing condition

$$x^+ \sim x^+ + h(\phi);$$

where, at the shock $x = 0, r = 1$, we have $x = e^{-t}$, $x = e^t$. Clearly, in order to preserve (7.1), we must have that

$$h(\phi + 2\pi) = h(\phi);$$

If we let E be the energy of the particle creating the shock and located at $\phi = 0$, the function $h(\phi)$ satisfies

$$\frac{\partial^2}{\partial \phi^2} h(\phi) = 16 G E \sum_n e^{i n \phi} \tag{7.3}$$

with $n \in \mathbb{Z}$, whose particular solution, satisfying the periodicity condition, is given by [30]

$$h(\phi) = 8 G E \sum_n e^{i n \phi} \tag{7.4}$$

In order to compute the two-point function across the shock, we must extend the results of section 3. Indeed, in section 4 we have used the invariance under translations in the Poincare patch $x > 0$ to place the source point p_1 at the origin $(0; 1; 0)$ of M^2 . This is clearly not general enough in the present context, since we are considering the quotient of M^2 by a boost. We must therefore consider the more general source point

$$p_1 = (e^t; e^{-t}; e; e);$$

where the last two entries explicitly denote the light cone coordinates on M^2 . Moreover, we must consider a source which is invariant under (7.1), so we must add all points p_1 with $! + Z$. We also define the probe point p_3 after the shock by

$$p_3 = (e^{t^0}; e^{t^0}; e^0; e^0);$$

where we parameterize the region with $x^- < 0$ and $x^+ > 0$ after the shock using (7.2) with the only change $x^- = e^{-t^0} r^2 - 1$. We then have that

$$2p_1 \cdot p_3 = 2 \cosh t^0 + 2 \cosh^0 :$$

Therefore, in the absence of a shock, the basic two-point function of a field of conformal dimension Δ is given by [19]

$$O_1(t;) O_1(t^0; ^0) = C_{\Delta} \frac{1}{2 \cosh(t - t^0) + 2 \cosh(\Delta + n^0)} : \quad (7.3)$$

On the other hand, when the gluing function $h(\cdot)$ is non-vanishing, we may use (4.7) to obtain directly the two-point function. More precisely, to obtain the vector q in (4.7) we first rescale $p_1 \rightarrow e^t p_1$ and $p_3 \rightarrow e^{t^0} p_3$ in order to rescale the p coordinates to 1. Then the vector q is the M^2 part of $e^{t^0} p_3 - e^t p_1$, which has light cone components $(e^{t^0 + ^0} + e^{t^+}; e^{t^0 - ^0} + e^{t^-})$. Summing over images of the initial source point, we then obtain the final result

$$O_1(t;) O_1(t^0; ^0)_{\text{shock}} = C_{\Delta} \frac{N_{\Delta} (2 - \Delta) e^{-\Delta(t+t^0)}}{2e^t \cosh(\Delta + n^0) + 2e^{t^0} \cosh(^0) + h(\cdot)^{\Delta - 1}} ;$$

which extends (7.3) to the full BTZ shock geometry. We shall leave a full exploration of the above result, including its relation to the full four-point function in the entangled thermal state of the CFT, for future research.

8. Future Work

This paper is a first step towards the understanding of the eikonal approximation in the context of the AdS/CFT correspondence. We were able to understand the AdS eikonal kinematical regime at tree level, relating the two-point function in the presence of a shock wave to the discontinuity across a kinematical branch cut of the dual CFT four-point function associated to the Witten diagram in figure 1(b). Thus, in order to fully reconstruct the four-point amplitude, extra information is needed: the monodromy alone is not enough. As such, the understanding of the full eikonal resummation is still missing and we leave it for future study. Nonetheless, in a companion paper [16] we explore the CFT consequences of the main result here obtained, and conjecture a possible resolution to the present problem concerning the reconstruction of the full four-point function.

Let us then conclude with other future directions of investigation:

All the discussion of this paper has been done for pure AdS. It is possible that the full discussion can be generalized to AdS compact spaces and to superspaces. This is important for applications of our results in the specific realizations of the AdS/CFT correspondence.

We have considered purely field theoretic interactions, neglecting all string effects. In flat space, on the other hand, it is known that, in the eikonal limit, the leading string effects simply Reggeize the gravitational interaction lowering its effective spin j from 2 to $2 + \alpha' t$. Reggeized interactions can then be resummed as usual. It would be important to include this leading correction in the context of AdS physics, following the work of [38, 39].

Eikonal formulae have an even greater range of validity in flat space, as shown in [11]. In the presence of a full string theoretic formulation of the interactions, the phase shift becomes an operator defining an explicitly unitary eikonal S-matrix. String effects are more than just Reggeization, but are still under control. The extension of these results to AdS would then be the next logical step, after the previous points have been understood.

It is of fundamental importance to extend the results of this paper to the BTZ geometry. In particular, one should be able to relate the two-point function computed in section 7 to a four-point function in the BTZ background. If this program can be carried to completion, it would yield information about thermal correlators at finite G , which should probe spacetime, and in particular the singularity, in a truly quantum gravity regime.

Finally, it would be of utmost importance to test all these results against computations performed directly in the CFT duals at finite N , possibly at weak coupling.

Acknowledgments

Our research is supported in part by INFN, by the MIUR-COFIN contract 2003{023852, by the EU contracts MRTN-CT-2004{503369, MRTN-CT-2004{512194, by the INTAS contract 03{51{6346, by the NATO grant PST.CLG.978785 and by the FCT contract POCTI/FNU/38004/2001. LC is supported by the MIUR contract "Rientro dei cervelli" part VII. MSC was partially supported by the FCT grant SFRH/BSAB/530/2005. JP is funded by the FCT fellowship SFRH/BD/9248/2002. Centro de Física do Porto is partially funded by FCT through the POCTI program.

A . P ropagators and C ontact n {P oint Functions

Let x, y be two points in AdS_{d+1} or H_{d+1} , satisfying $x^2 = y^2 = 1$. Define the chordal distance

$$z = \frac{1}{4} (x - y)^2 = \frac{1}{2} (1 + x \cdot y) :$$

The scalar propagator $\mathcal{G}(x; y)$ of a scalar field of mass m , normalized to

$$\begin{aligned} AdS_{d+1} \quad m^2 \quad \mathcal{G}(x; y) &= i \quad \mathcal{G}(x; y) ; & (\text{on } AdS_{d+1}) ; \\ H_{d+1} \quad m^2 \quad \mathcal{G}(x; y) &= \quad \mathcal{G}(x; y) ; & (\text{on } H_{d+1}) ; \end{aligned}$$

is given explicitly by

$$= \frac{1}{(4)^{\frac{d+1}{2}}} \frac{(\quad)}{(2 \quad d+1)} \frac{1}{(\quad z)} F \quad ; \frac{2 \quad d+1}{2} ; 2 \quad d+1 \frac{1}{z} ;$$

where Δ is the conformal dimension of the dual boundary operator $\Delta = d + \sqrt{d^2 + 4m^2}$. In particular, in this paper, we shall mostly denote with $\mathcal{G}(x; y)$ the Minkowskian massless propagator in AdS_{d+1} and with $\mathcal{G}(x; y)$ the Euclidean massive propagator on H_{d+1} of conformal dimension $\Delta - 1$. They are explicitly given by

$$= \frac{\frac{d+1}{2}}{d (4)^{\frac{d+1}{2}}} \frac{1}{(\quad z)^\Delta} F \quad d; \frac{d+1}{2}; d+1 \frac{1}{z}$$

and by

$$= \frac{\frac{d+1}{2}}{d(d-1) (4)^{\frac{d+1}{2}}} \frac{1}{(\quad z)^{\Delta-1}} F \quad d-1; \frac{d+1}{2}; d+1 \frac{1}{z} :$$

We also introduce the contact n -point functions

$$D^d_i(p_i) = \int_{H_{d+1}} d^d y \int_Z \frac{1}{(\quad 2y_{ij} p_i)}$$

They are given by the integral representation

$$\begin{aligned} D^d_i(p_i) &= \frac{\frac{d}{2}}{(\quad i)} \int_Z \int_{\mathbb{Q}} dt_i t_i^{i-1} e^{\frac{1}{2} \sum_{i,j} t_i t_j p_{ij}} \\ &= \frac{\frac{d}{2}}{2} \frac{\frac{d}{2}}{(\quad i)} \int_Z \int_{\mathbb{Q}} dt_i t_i^{i-1} \frac{(\quad i t_i - 1)}{\frac{1}{2} \sum_{i,j} t_i t_j p_{ij}} ; \end{aligned}$$

with $\Delta = \frac{d}{2} + i$ and with $p_{ij} = 2p_i \cdot p_j$. The two-point function integral can be explicitly computed as

$$D^d_{1;2}(p_1; p_2) = \frac{1}{p_1^2 - \frac{1}{2}} \frac{\frac{d}{2}}{p_2^2 - \frac{1}{2}} \frac{1}{2} \frac{\frac{d}{2}}{(\quad)} {}_2F_2 \left(\frac{d}{2}; \frac{d}{2}; 1 \quad \frac{1}{2} \right) ;$$

where

$$+ \frac{1}{2} = \frac{2p_1 \cdot p_2}{p_1^2 - \frac{1}{2} p_2^2 - \frac{1}{2}} :$$

Moreover, as shown in [35], the four-point function $D^d_{2;2;1;1}$ can be explicitly computed in terms of standard one loop box integrals, as reviewed in section 6.1.

B. Explicit Computations in Poincare Coordinates

The reader who is familiar with the calculation of correlation functions in AdS in, e.g., [5, 3, 24], will find in the present appendix a pedagogical and very explicit introduction to the calculations of the shock two-point function performed in the bulk of the paper.

Let us recall two standard sets of coordinates in AdS_{d+1} . We first have the usual Poincare coordinates $(z; z^\mu)$, parameterizing the Poincare patch $x^0 > 0$. They are defined by

$$x^\mu = \frac{1}{z} (z^2 + z^\mu z^\mu); 1; z^\mu ;$$

with the AdS metric taking the standard conformally flat form

$$ds^2(AdS_{d+1}) = \frac{dz^2 + dz^\mu dz^\mu}{z^2} ;$$

Another useful set of coordinates, parameterizing the region $x^0 = x^1 = 1 < 0$ near the shock, is given by null coordinates $(u^+; u^-; u^\mu)$ with $u^\mu \in H_{d-1}$, where now

$$\begin{aligned} x^+ &= \frac{4u^+}{4 + u^+ u^-} ; & x^- &= \frac{4u^-}{4 + u^+ u^-} ; \\ x^\mu &= \frac{4}{4 + u^+ u^-} u^\mu ; \end{aligned} \tag{B.1}$$

Here, u^μ denotes a point along the transverse hyperboloid, which is parameterized in general by $d-1$ angular variables. The AdS metric now reads

$$ds^2(AdS_{d+1}) = \frac{16du^+ du^-}{(4 + u^+ u^-)^2} + \frac{4}{4 + u^+ u^-} ds^2(H_{d-1}) ;$$

with volume form given by

$$dAdS_{d+1} = 8 \frac{(4 - u^+ u^-)^{d-1}}{(4 + u^+ u^-)^{d+1}} du^+ du^- dH_{d-1} ; \tag{B.2}$$

We shall mostly work in $d=2$, where

$$u^0 = u^1 = e^\pm ; \quad ds^2(H_1) = d\varphi^2 ; \quad H_1 = S^1 ;$$

We now recall the standard computation of the AdS boundary two-point function, starting with Poincare coordinates. We parameterize points on the boundary as always with p_μ , where the boundary point is given in global embedding coordinates by

$$p_\mu = (p_0, p_1; 1; p_\mu) ;$$

Since

$$2p_0 = \frac{1}{z} (z^2 + (z^\mu - p_\mu)^2)$$

we obtain the usual expression for the bulk-to-boundary propagator

$$K(z; z_0; p_1) = C \frac{z^d}{z^2 + (z - p_1)^2} \quad ;$$

Given boundary data $\phi_0(p_1)$, the bulk scalar field value is given in terms of the propagator by [3, 24]

$$\phi(z; z_0) = \int d^d p_1 K(z; z_0; p_1) \phi_0(p_1) ;$$

Throughout the paper, the propagator K is taken to be the limit of the bulk-to-boundary propagator, and its normalization differs from the standard one in the literature [5, 3] by a factor of 2^{d-1} . Therefore $\lim_{z \rightarrow 0} z^{d-1} \phi(z; z_0) = (2^{d-1})^{-1} \phi_0(z_0)$. Moreover, the two-point function is given by

$$\langle \phi_0(p_1) \phi_0(p_2) \rangle = \frac{(2^{d-1})^{-1}}{i} \lim_{z \rightarrow 0} \int d^d z \int d^d p_1 \frac{\partial}{\partial z} K(z; z_0; p_1) \frac{\partial}{\partial z} K(z; z_0; p_2) \quad ;$$

and it follows that

$$\langle \phi_0(p_1) \phi_0(p_2) \rangle = \frac{C}{p_1 \cdot p_2} \quad ; \tag{B.3}$$

Recall that [24] the coefficient $(2^{d-1})^{-1}$ arises from a careful treatment of regularization at the boundary.

In the following we shall compute the two-point function, in the presence of the shock wave, using null coordinates. It is then instructive to repeat the calculation above in these coordinates. A point on the boundary with $u^+ u^- = 4$ is given by

$$p_1 = \left(\frac{2}{u_1}, \frac{u_1}{2}, u_1, \dots \right) ;$$

and the bulk-to-boundary propagator is now given by

$$\frac{C}{(2p \cdot x)} = C \frac{(4 + u^+ u^-) u_1 u_2}{2u^+ u^- u_1^2 \cdot 8(u^-)^2 \cdot 2(4 - u^+ u^-) u_1 u_2 \cdot u_1 u_2} \quad ;$$

Sending the point x to p_2 on the boundary one obtains the two-point function in null coordinates as

$$\langle \phi(u_1; u_1) \phi(u_2; u_2) \rangle = C \frac{u_1 u_2}{u_1 u_1 \cdot u_2 u_2} \quad ;$$

In the presence of a shock the original metric in null coordinates gains an additional term

$$ds^2 (AdS_3) + du^2 + u h(\dots) ;$$

where from now on we specialize to the case $d = 2$ for concreteness. Recall that the function $h(\dots)$ satisfies

$$\frac{\partial^2}{\partial^2} h(\dots) = 16 G(\dots) ;$$

so that the particular solution satisfying $\lim_{z \rightarrow 1} h(z) = 0$ is given by

$$h(z) = 8 G^2 e^{-2z}.$$

We now have all the required data in order to proceed with the calculation of the two-point function in the AdS shock wave background. The geometry is described by a metric $g_{mn} + g_{sh}^n$, where only g is non-vanishing and where $g_{sh}^n = 0$. Therefore, the volume form is insensitive to g_{sh}^n and is given by $\sqrt{-g}$ in (B.2). One can also compute the inverse metric, $(g + g_{sh}^n)^{mn} = g^{mn} - g_{sh}^n$, with single non-vanishing component $g^{++} = 4(u)h(z)$. The action for a scalar field in the AdS shock wave background is then

$$S[\phi] = S_0[\phi] + \frac{1}{2} \int_{\mathcal{Z}} \sqrt{-g} \delta g_{mn} \partial_m \phi \partial_n \phi$$

where $S_0[\phi]$ is the standard AdS action for a scalar field, and the new term has support on the shock wave alone, as it includes a delta function restricting it to $u = 0$. This new term is what we shall call the shock wave vertex; it is a new 2-vertex needed to compute the two-point function in the AdS shock wave background, and it is precisely located at the position of the shock wave. It is given explicitly by

$$\int_{\mathcal{Z}} du^+ d^2x \delta h(z) \delta_+(x - x_+) \delta_+(x - x_-)$$

One may now compute the leading correction to the two-point function (B.3) in the AdS shock wave background. At a graphical level this is rather simple: the leading graph includes two boundary-to-bulk propagators, which meet at the shock wave 2-vertex; the higher order graphs includes two boundary-to-bulk propagators, and n different shock wave 2-vertices connected by $n-1$ bulk-to-bulk propagators. The leading correction is simply given by

$$2C^2 \int_{\mathcal{Z}} du^+ d^2x \delta h(z) \delta_+(x - x_+) \delta_+(x - x_-)$$

where x is given explicitly in terms of u ; u in (B.1) and where the boundary points p_1, p_2 are explicitly given by $p_1 = (p_1^+, p_1^-, 1; p_1)$ and $p_2 = (p_2^+, p_2^-, 1; p_2)$. Working always in null coordinates, and using that, along the shock at $u = 0$ we have

$$\delta_+(x - x_+) = \frac{i}{(2\pi)^2} \int_{\mathcal{Z}} ds_1 s_1^{-1} e^{is_1(u^+ - 2u^-)};$$

$$\delta_+(x - x_-) = \frac{i}{(2\pi)^2} \int_{\mathcal{Z}} ds_2 s_2^{-1} e^{is_2(u^+ + 2u^-)};$$

we obtain

$$2C^2 \frac{i^2}{(2\pi)^2} \int_{\mathcal{Z}} ds_1 ds_2 s_1^{-1} s_2^{-1} \int_{\mathcal{Z}} du^+ d^2x \delta h(z) e^{i(s_1 - s_2)u^+} e^{2i(s_2 p_2^- - s_1 p_1^-)u^-}$$

Integrating in u^+ we obtain $2\pi \delta(s_1 - s_2)$ and therefore we finally get

$$4 C^2 \frac{i^2}{(2\pi)^2} \int_{\mathcal{Z}} ds s^{-2} \int_{\mathcal{Z}} d^2x \delta h(z) e^{2is(p_2^- - p_1^-)u^-}$$

$$= 2 C N \int_{\mathcal{Z}} d^2x \frac{h(z)}{[2(p_2^- - p_1^-)u^-]^2};$$

which matches exactly the result (5.1) in the bulk of the paper. In this particular two-dimensional case one may further compute explicitly the integral as

$$G = \int_{-Z}^Z \frac{e^{-j^2}}{[q e^{j^2} + 1]^{2+1}} ;$$

where

$$q = p_2^0 - p_1^0 - p_2^1 - p_1^1 ;$$

Computing the integral one obtains the result (here F is the standard ${}_2F_1$ hypergeometric function),

$$G = \frac{8^{-2} C_N (2+1)}{(2+1)} \left[\frac{1}{(q)^{2+1}} F\left(\begin{matrix} - \\ +1; 2+1; +2 \end{matrix} \middle| \frac{q}{q} \right) + \frac{1}{(q)^{2+1}} F\left(\begin{matrix} - \\ +1; 2+1; +2 \end{matrix} \middle| \frac{q}{q} \right) \right] ;$$

In order to proceed to higher orders in G , obtaining the exact two-point function in the AdS shock wave background, we would need to compute graphs with an arbitrary number of shock wave vertices. On the other hand, this immediately poses a problem in the calculation. A general graph includes bulk to bulk propagators between the vertices which are positioned along the shock surface. Since the geodesic distance of two points along the shock is insensitive to the v coordinate, the naive computation of the graph produces divergences coming from the integrations along the light cone coordinate v . This means that, in order to compute higher order contributions to the shock wave two-point function, one first needs to devise a suitable regularization of these graphs. In section 4 we have solved this problem using a generalization of the technique introduced by 't Hooft in [9].

References

- [1] J.M. Maldacena, The Large N Limit of Superconformal Field Theories and Supergravity, *Adv. Theor. Math. Phys.* 2 (1998) 231, [arXiv:hep-th/9711200].
- [2] S.S. Gubser, I.R. Klebanov and A.M. Polyakov, Gauge Theory Correlators from Noncritical String Theory, *Phys. Lett. B* 428 (1998) 105, [arXiv:hep-th/9802109].
- [3] E. Witten, Anti-de Sitter Space and Holography, *Adv. Theor. Math. Phys.* 2 (1998) 253, [arXiv:hep-th/9802150].
- [4] O. Aharony, S.S. Gubser, J.M. Maldacena, H. Ooguri and Y. Oz, Large N Field Theories, String Theory and Gravity, *Phys. Rept.* 323 (2000) 183, [arXiv:hep-th/9905111].
- [5] E. D'Hoker and D.Z. Freedman, Supersymmetric Gauge Theories and the AdS/CFT Correspondence, [arXiv:hep-th/0201253].
- [6] E. D'Hoker, D.Z. Freedman, S.D. Mathur, A. Matusis and L. Rastelli, Graviton Exchange and Complete 4-Point Functions in the AdS/CFT Correspondence, *Nucl. Phys. B* 562 (1999) 353, [arXiv:hep-th/9903196].
- [7] E. D'Hoker, S.D. Mathur, A. Matusis and L. Rastelli, The Operator Product Expansion of $N = 4$ SYM and the 4-Point Functions of Supergravity, *Nucl. Phys. B* 589 (2000) 38, [arXiv:hep-th/9911222].
- [8] M. Levy and J. Sucher, Eikonal Approximation in Quantum Field Theory, *Phys. Rev.* 186 (1969) 1656.
- [9] G. 't Hooft, Graviton Dominance in Ultrahigh Energy Scattering, *Phys. Lett. B* 198 (1987) 61.
- [10] D. Kabat and M. Ortiz, Eikonal Quantum Gravity and Planckian Scattering, *Nucl. Phys. B* 388 (1992) 570, [arXiv:hep-th/9203082].
- [11] D. Amati, M. Ciafaloni and G. Veneziano, Superstring Collisions at Planckian Energies, *Phys. Lett. B* 197 (1987) 81.
- [12] G. 't Hooft, Nonperturbative Two Particle Scattering Amplitudes in $(2 + 1)$ -Dimensional Quantum Gravity, *Commun. Math. Phys.* 117 (1988) 685.
- [13] S. Deser and R. Jackiw, Classical and Quantum Scattering on a Cone, *Commun. Math. Phys.* 118 (1988) 495.
- [14] S. Deser, J.G. McCarthy and A.R. Steif, Ultra-Planck Scattering in $D = 3$ Gravity Theories, *Nucl. Phys. B* 412 (1994) 305, [arXiv:hep-th/9307092].
- [15] P.C. Aichelburg and R.U. Sexl, On the Gravitational Field of a Massless Particle, *Gen. Rel. Grav.* 2 (1971) 303.
- [16] L. Comalba, M.S. Costa, J. Penedones and R. Schiappa, Eikonal Approximation in AdS/CFT: Conformal Partial Waves and Finite N Four-Point Functions, [arXiv:hep-th/0611123].
- [17] M. Banados, C. Teitelboim and J. Zanelli, The Black Hole in Three-Dimensional Spacetime, *Phys. Rev. Lett.* 69 (1992) 1849, [arXiv:hep-th/9204099].
- [18] M. Banados, M. Henneaux, C. Teitelboim and J. Zanelli, Geometry of the $(2 + 1)$ Black Hole, *Phys. Rev. D* 48 (1993) 1506, [arXiv:gr-qc/9302012].
- [19] P. Kraus, H. Ooguri and S. Shenker, Inside the Horizon with AdS/CFT, *Phys. Rev. D* 67 (2003) 124022, [arXiv:hep-th/0212277].
- [20] L. Filkowski, V. Hubeny, M. Kleban and S. Shenker, The Black Hole Singularity in AdS/CFT, *JHEP* 0402 (2004) 014, [arXiv:hep-th/0306170].
- [21] G. Festuccia and H. Liu, Excursions Beyond the Horizon: Black Hole Singularities in Yang-Mills Theories I, *JHEP* 0604 (2006) 044, [arXiv:hep-th/0506202].

- [22] J.F. Barber and E. Rabinovici, Very Long Time Scales and Black Hole Thermal Equilibrium, *JHEP* 0311 (2003) 047, [arXiv:hep-th/0308063].
- [23] V.E. Hubeny, H. Liu and M. Rangamani, Bulk{Cone Singularities & Signatures of Horizon Formation in AdS/CFT, [arXiv:hep-th/0610041].
- [24] D.Z. Freedman, S.D. Mathur, A. Matusis and L. Rastelli, Correlation Functions in the CFT_d/AdS_{d+1} Correspondence, *Nucl. Phys. B* 546 (1999) 96, [arXiv:hep-th/9804058].
- [25] F.A. Dolan and H. Osborn, Conformal Partial Waves and the Operator Product Expansion, *Nucl. Phys. B* 678 (2004) 491, [arXiv:hep-th/0309180].
- [26] F.A. Dolan and H. Osborn, Conformal Four{Point Functions and the Operator Product Expansion, *Nucl. Phys. B* 599 (2001) 459, [arXiv:hep-th/0011040].
- [27] T. Dray and G. 't Hooft, The Gravitational Shock Wave of a Massless Particle, *Nucl. Phys. B* 253 (1985) 173.
- [28] M. Hotta and M. Tanaka, Shock Wave Geometry with Non{Vanishing Cosmological Constant, *Class. Quant. Grav.* 10 (1993) 307.
- [29] J. Podolsky and J.B. Gri ths, Impulsive Gravitational Waves Generated by Null Particles in de Sitter and Anti{de Sitter Backgrounds, *Phys. Rev. D* 56 (1997) 4756.
- [30] K. Sfetsos, On Gravitational Shock Waves in Curved Spacetimes, *Nucl. Phys. B* 436 (1995) 721, [arXiv:hep-th/9408169].
- [31] G.T. Horowitz and N. Itzhaki, Black Holes, Shock Waves and Causality in the AdS/CFT Correspondence, *JHEP* 9902 (1999) 010, [arXiv:hep-th/9901012].
- [32] G. Arcioni, S. de Haro and M. O'Loughlin, Boundary Description of Planckian Scattering in Curved Spacetimes, *JHEP* 0107 (2001) 035, [arXiv:hep-th/0104039].
- [33] I.R. Klebanov and E. Witten, AdS/CFT Correspondence and Symmetry Breaking, *Nucl. Phys. B* 556 (1999) 89, [arXiv:hep-th/9905104].
- [34] E. D'Hoker, D.Z. Freedman and L. Rastelli, AdS/CFT 4{Point Functions: How to Succeed at z{Integrals Without Really Trying, *Nucl. Phys. B* 562 (1999) 395, [arXiv:hep-th/9905049].
- [35] M. Bianchi, M.B. Green, S. Kovacs and G. Rossi, Instantons in Supersymmetric Yang{Mills and D{Instantons in IIB Superstring Theory, *JHEP* 9808 (1998) 013, [arXiv:hep-th/9807033].
- [36] J. Maldacena, Eternal Black Holes in Anti{de Sitter, *JHEP* 0304 (2003) 021, [arXiv:hep-th/0106112].
- [37] H. Muller-Kirsten, N. Ohta and J-G. Zhou, AdS₃/CFT Correspondence, Poincare Vacuum State and Greybody Factors in BTZ Black Holes, *Phys. Lett. B* 445 (1999) 287, [arXiv:hep-th/9809193].
- [38] R.C. Brower, J. Polchinski, M.J. Strassler and C.I. Tan, The Pomeron and Gauge/String Duality, [arXiv:hep-th/0603115].
- [39] J. Polchinski and M.J. Strassler, Hard Scattering and Gauge/String Duality, *Phys. Rev. Lett.* 88 (2002) 031601, [arXiv:hep-th/0109174].